Efficient Synthesis and Photodynamic Activity of Porphyrin-Saccharide Conjugates: Targeting and Incapacitating Cancer Cells†

Xin Chen,‡ Li Hui,§ David A. Foster,§ and Charles Michael Drain*,‡,||

Department of Chemistry and Biochemistry and Department of Biological Science, Hunter College and the Graduate Center of the City University of New York, 695 Park Avenue, New York, New York 10021, and The Rockefeller University, 1230 York Avenue, New York, New York 10021

Received April 12, 2004; Revised Manuscript Received June 4, 2004

ABSTRACT: Since the role of saccharides in cell recognition, metabolism, and cell labeling is well-established, the conjugation of saccharides to drugs is an active area of research. Thus, one goal in the use of saccharide-drug conjugates is to impart a greater specificity toward a given cell type or other targets. Although widely used to treat some cancers and age related macular degeneration, the drugs used in photodynamic therapy (PDT) display poor chemical selectivity toward the intended targets, and uptake by cells most likely arises from passive, diffusional processes. Instead, the specific irradiation of the target tissues, and the formation of the toxic species in situ, are the primary factors that modulate the selectivity in the present mode of PDT. We report herein a two-step method to make nonhydrolyzable saccharide−porphyrin conjugates in high yields using a tetra(pentafluorophenyl)porphyrin and the thio derivative of the sugar. As a demonstration of their properties, the selective uptake (and/or binding) of these compounds to several cancer cell types was examined, followed by an investigation of their photodynamic properties. As expected, different malignant cell types take up one type of saccharide−porphyrin conjugate preferentially over others; for example, human breast cancer cells (MDA-MB-231) absorb a tetraglucose−porphyrin conjugate over the corresponding galactose derivative. Doseametric studies reveal that these saccharide−porphyrin conjugates exhibit varying PDT responses depending on drug concentration and irradiation energy. (1) Using 20 μM conjugate and greater irradiation energy induces cell death by necrosis. (2) When 10−20 μM conjugate and less irradiation energy are used, both necrosis and apoptosis are observed. (3) Using 10 μM and the least irradiation energy, a significant reduction in cell migration is observed, which indicates a reduction in aggressiveness of the cancer cells.

The uptake of exogenous molecules such as drugs into cells can arise from a variety of mechanisms that can be broadly classified as active and passive transport. Active uptake requires that target molecules be recognized by specific intermolecular interactions, selected, and shuttled across the cell membrane by receptors. Thus, molecules may be targeted toward these receptors by appending appropriate substrate moieties. Conversely, passive uptake involves diffusion at some point in the process and arises from nonspecific cell−molecule interactions. Because of the lipid membrane core, the more lipophilic a molecule, the lower the barrier to traversing through the cell membrane, whereas amphipathic molecules will nominally bind at the interface or polar region and have greater barriers to crossing the membrane (*1*, *2*).

Photodynamic therapy (PDT)[1] is a rapidly growing methodology to treat age-related macular degeneration, various skin disorders, and an increasing number of cancers that are accessible to irradiation with visible light (*3*). Although in various stages of development, other applications are envisaged; for example, as antibiotic and antiviral treatments (*4*, *5*). A benzoporphyrin derivative is used in the treatment of age-related macular degeneration (*6*) and the PDT agent photofrin, which is approved for use in a variety of cancers, is a complex mixture of hematoporphyrin IX oligomers with issues of dosaging and selectivity (*7*). There are several other porphyrinoid derivatives and related compounds that are in various phases of testing and in clinical trials for both treatment and imaging applications, including chlorins (reduced porphyrins) and texaphyrins (expanded porphyrins) (*8*−*10*).

† The authors acknowledge support from the National Institutes of Health (NIH)-SCORE program (GM60654) to C.M.D. and D.A.F.; the PSC-CUNY fund and National Science Foundation (CHE-0135509) to C.M.D.; and the National Cancer Institute (CA46677) to D.A.F. Research Centers in Minority Institutions Award RR-03037 from the National Center for Research Resources of the National Institutes of Health, which partially supports infrastructure and instrumentation in the sciences at Hunter College, is also acknowledged.

* To whom correspondence should be addressed. E-mail: cdrain@hunter.cuny.edu. Phone: (212) 650-3791. Fax: (212) 772-5332.

‡ Department of Chemistry and Biochemistry, Hunter College.

§ Department of Biological Science, Hunter College.

|| Rockefeller University.

[1] Abbreviations: PDT, photodynamic therapy; P-Glu$_4$, 5,10,15,20-tetrakis(4,1′-thio-glucose-2,3,5,6-tetrafluorophenyl)porphyrin; P-Gal$_4$, 5,10,15,20-tetrakis(4,1′-thio-galactose-2,3,5,6-tetrafluorophenyl)porphyrin; DMEM, Dulbecco's Modified Eagle Medium; PARP, poly-(ADP ribose) polymerase; TPPF$_{20}$, 5,10,15,20-tetrakis(pentafluorophenyl)-porphyrin; ESI-MS, electron spray ionization mass spectroscopy; TPP, tetraphenylporphyrin.

10.1021/bi049272v CCC: $27.50
Published on Web 07/28/2004

Scheme 1: Structures of P-Glu_4 and P-Gal_4

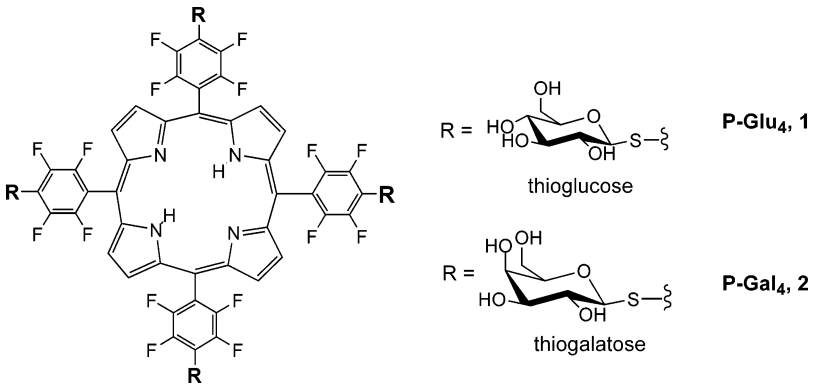

In general terms, the PDT concept is that the therapeutic compound has low toxicity until it is activated by light, whereupon it becomes very reactive and toxic or it activates other indigenous species to become reactive and toxic (*6*, *7*, *11*). The selectivity in any application arises from the compound specificity for the target and the selective irradiation of the target by light. Specificity for target tissues is poor for most PDT agents and arises largely from nonspecific passive uptake modulated by increased metabolic activity of cancer cells—as demonstrated by the strong correlation between hydrophobicity and in vitro activity. For PDT applications, there is a general agreement that the major role of porphyrinoid compounds is to photosensitize the formation of the highly reactive singlet oxygen species via a transfer of energy from the triplet excited state of the porphyrinoid to ground state, triplet oxygen. Singlet oxygen is a powerful oxidant that reacts with many biomolecular species such as the double bonds in lipids, aromatic amino acids, both phosphate backbone and bases of nucleic acids, and other species such as flavenoids. Enzymes designed to reduce oxidative stress such as superoxide dismutase and antioxidants may reduce the amounts of singlet oxygen in the cell and thereby modulate PDT efficiency. In some cases, PDT may cause cell death by making the cells anoxic or by the initiation of apoptosis. Most porphyrins have remarkably high quantum yields for triplet formation, >60%. The yield of the triplet state can be increased by the incorporation of some metals into the core and/or by replacing some of the hydrogen atoms with halogens or other heavy atoms that enhance intersystem crossing from the initially formed singlet state to the triplet state. Since fluorinated porphyrin derivatives generally have greater triplet quantum yields than most free base porphyrinic systems (*12*); these compounds may be more potent photosensitizers.

Because of the poor selectivity for target tissue, dosing concerns, and the large market, much effort has been directed toward the discovery and implementation of the next generation of PDT agents (*3*, *8*, *13*−*15*). Despite these research efforts and a better understanding of how the present photofrin mixture works, there is a paucity of progress in making porphyrinoid compounds more selective for the target tumor tissues, yet stable in vivo. Although the role of lipophilicity in enhancing PDT activity is not well-understood, it likely arises from enhanced affinity for cell membranes and concomitant increased cellular uptake due to the lower energetic costs of traversing the low dielectric of the membrane (*1*, *2*, *16*). Liposomes and nanoparticles are a means to circumvent solubility problems, and many new compounds under investigation are amphipathic or hydrophobic, but selectivity remains an issue (*17*). A cadre of glycosylated porphyrins has been reported in recent years (*18*−*23*) because of the advantages of appending cellular recognition elements to a drug, yet hydrolysis of the sugars from the *O*-glycosidic porphyrin derivatives remains problematic—both in vivo and during synthesis/purification (*24*). Drugs bearing saccharides appended via *O*-glycoside linkages generally have short half-lives because this bond is readily hydrolyzed by a variety of enzymatic and nonenzymatic acid/base reactions. Most cancer cells are dependent on glucose uptake to fulfill their energy requirements; as such, glycolysis is increased in cancer cells as compared with normal cells. Glucose enters cells via a family of functional glucose transporters. In this regard, breast cancer cells are not exceptional and are known to have increased glucose utilization and uptake due to an increased number of transporters (*25*). Porphyrins with several sugar moieties at appropriate positions can be amphipathic to facilitate passive uptake, and the sugars may mediate specific interactions with cancer cell membranes and active uptake of the compound (*26*). To surmount the hydrolysis problem, saccharide−drug conjugates using *C*- or *S*-glycoside linkages have been made, including several porphyrin derivatives (*23*, *27*−*30*), but for the majority of cases, the synthetic yield of these conjugates is poor as well.

To address many of the aforementioned issues of selectivity, amphipathicity, and hydrolytic stability in the design and efficacy of drugs such as those for PDT, we report herein the synthesis and the manifold activities of two porphyrin−saccharide conjugates (Scheme 1): 5,10,15,20-tetrakis(4,1′-thio-glucose-2,3,5,6-tetrafluorophenyl)porphyrin (P-Glu_4) and 5,10,15,20-tetrakis(4,1′-thio-galactose-2,3,5,6-tetrafluorophenyl)porphyrin (P-Gal_4). A simple, two-step reaction affords a porphyrin bearing four saccharide moieties conjugated via an *S*-glycoside bond in high yields (Scheme 2). The reaction is general for a variety of saccharides and other nucleophiles such as amines.

These porphyrin−*S*-saccharide derivatives exhibit enhanced binding to a human breast cancer cell line as compared to several widely studied nonsaccharide derivatives, such as the tetra(4-methoxyphenyl)porphyrin (Supporting Information). These studies also show that the glucose-appended porphyrin is preferentially taken up as compared to the galactose-appended derivative, wherein it displays significantly enhanced photodynamic activity in

Scheme 2: Thioacetate Sugar Derivative (A) Is More Stable than the Free Thiol. (B) Synthesis of P-Glu_4 and P-Gal_4 Can Be Accomplished Using the Protected Sugar Followed by Deprotection or Directly by Using the Unprotected Sugar (C)

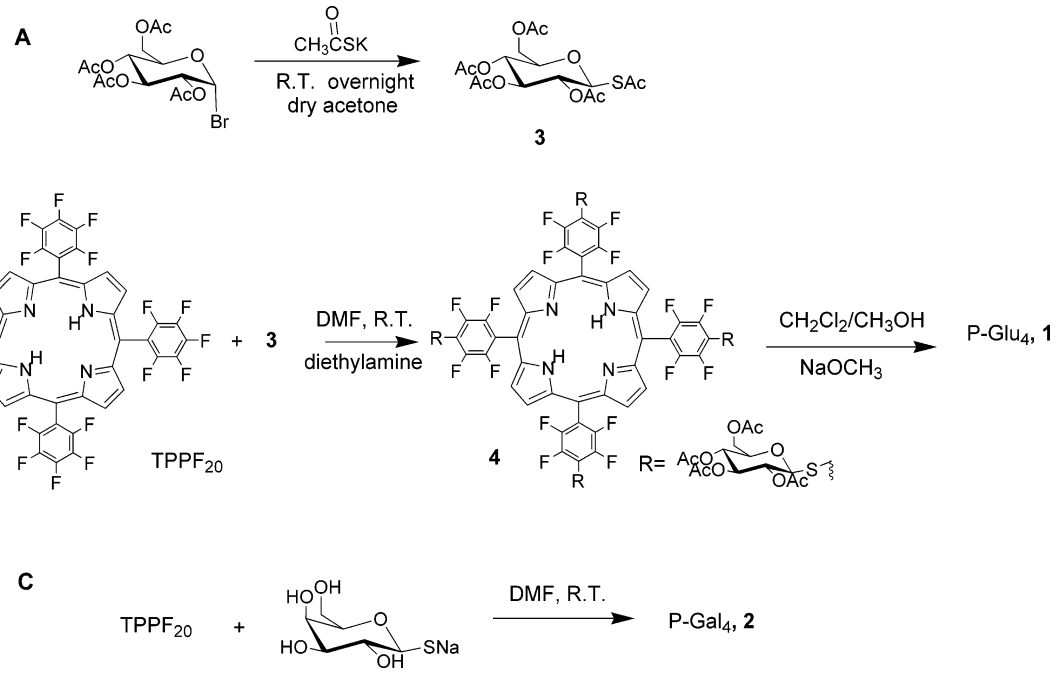

terms of inducing necrosis and apoptosis. Studies reveal that the cellular responses are dependent on the dosage of these compounds, length of irradiation with white light, and the degree of uptake. The 20 μM doses of P-Glu_4 and ~11.3 kJ m^{-2} (20 min at 0.94 mW cm^{-2} irradiation using white light from a ~13 W fluorescent bulb) result in necrosis. The 20 μM doses of the same derivative and ~1.6 kJ m^{-2} (10 min at 0.27 mW cm^{-2}) irradiation results in apoptosis. Still lower concentrations and shorter irradiation times, 10 μM doses of P-Glu_4 and 0.75 kJ m^{-2} (5 min at 0.25 mW cm^{-2}), significantly reduce cell mobility, which is an indicator of reduced aggressiveness. Also, a normal rat fibroblast cell line absorbs less of the conjugates than the transformed version of the cell line.

EXPERIMENTAL PROCEDURES

Materials. All chemicals were purchased from Sigma-Aldrich. Dulbecco's Modified Eagle Medium (DMEM) and antimycotic for cell culture were from GibcoBRL. Bovine calf serum was obtained from HyClone. PBS was obtained from Invitrogen. The 13 W fluorescent bulb was from Sanco. The antibody against poly-(ADP ribose) polymerase (PARP) was from Cell Signaling Technology. Biocoat filters were purchased from Becton Dichinson Labware, and the Diff-Quik stain set was from Dade Behring Inc.

Instrumentation. Steady-state fluorescence spectra were generally taken on 1 μM porphyrin in methanol, with excitation at the maximum UV−vis absorbance (Soret band), and recorded on a Fluorolog 3, Jobin-SPEX Instruments S. A., Inc. UV−vis spectra were collected on a Varian Bio3 spectrophotometer. Flash column chromatography was performed using 230−400 mesh ASTM Merck silica gel-60. ^{1}H NMRs were recorded on a Varian 300 MHz instrument in $CDCl_3$. Electron spray ionization mass spectrometry used an Aligent Technologies HP-1100 LC/MSD instrument.

*Porphyrin Synthesis and Characterization. 5,10,15,20-Tetrakis(4-1′-thio-glucosyl-2,3,5,6-tetrafluorophenyl)porphyrin (P-Glu_4, **1**).* 2,3,4,6-Tetra-*O*-acetyl-glucosyl bromide (7.0 g, 0.017 mol) mixed with potassium thioacetate (4.0 g, 0.035 mol) in 20 mL of dry acetone overnight at room temperature afforded 2,3,4,6-tetra-*O*-acetyl-glucosyl thioacetate (**3**) after removal of the solvent and purification over a 5 × 20 cm silica gel column using hexane/ethyl acetate (2:1) as eluent. A 8:1 solution of **3** (167 mg, 410.4 μmol) and 5,10,15,20-tetrakis(pentafluorophenyl)porphyrin ($TPPF_{20}$) (50 mg, 51.3 μmol) in 10 mL of DMF was stirred overnight at room temperature to yield 5,10,15,20-tetrakis(4-1′-thio-2′,3′,4′,6′-tetraacetylglucosyl-2,3,5,6-tetrafluorophenyl)porphyrin (**4**). Compound **4** was purified by column chromatography using 2 × 15 cm silica gel column hexane/ethyl acetate (2:3) as eluent, treated with 16 equiv (1 equiv per acetate group) of $NaOCH_3$ at room temperature in 9:1 v/v solution of methanol/methylene chloride for 1 h to afford P-Glu_4 in quantitative yield (Scheme 2). The product was neutralized by pH 7.2 ammonium acetate buffer. The overall yield after three steps was 88%. P-Glu_4: UV−vis in methanol $\lambda(\epsilon$ cm^{-1} $M^{-1})$, 410 nm (1.83×10^5). Alternatively, the unprotected sodium thioglucose can be used as a starting material to make **1**, as described next for the galactose derivative.

5,10,15,20-Tetrakis(4-1′-thio-galactosyl-2,3,5,6-tetrafluorophenyl)porphyrin (P-Gal_4, **2**) was synthesized as described previously (*24*) (Scheme 2) by stirring a 8:1 solution of the sodium thiogalactose (54 mg, 246.4 μmol) with $TPPF_{20}$ (30 mg, 30.8 μmol), respectively, in 5 mL of DMF at room temperature overnight and purified over a 1 × 10 cm silica gel column using ethyl acetate/methanol (17:3) as eluent. The yield was 92%. To accurately characterize the compounds by NMR, the tetra-2,3,4,6-acetylgalactose derivatives were synthesized by mixing acetic anhydride (84.4 mg, 78 μL, 826.2 μmol), DMAP (9 mg, 73.4 μmol), and P-Gal_4 (10 mg, 45.9 μmol) (48:1.6:1) at room temperature in 10 mL pyridine for 1 h to afford 5,10,15,20-tetrakis(4-1′-thio-2′,3′,4′,6′-tetraacetylgalactosyl-2,3,5,6-tetrafluorophenyl) porphyrin (**5**). Compound **5** was purified by column chroma-

tography using a 1 × 8 cm silica gel column and hexane/ethyl acetate (1:2) as eluent. When **5** was made directly, deprotection was accomplished using 16 equiv of $NaOCH_3$ (1 equiv per acetate group) at room temperature in 9:1 v/v solution of methanol/methylene chloride for 1 h to afford P-Gal_4 in quantitative yield (Scheme 2). The product was neutralized by pH 7.2 ammonium acetate buffer. P-Gal_4: UV−visible in methanol $\lambda(\epsilon\ cm^{-1}\ M^{-1})$, 410 nm ($1.74 \times 10^4$).

For compounds **4** and **5**, electron spray ionization mass spectrometry, ^1H NMR, UV−vis, and fluorescence spectra were consistent with the reported structures. For compounds **1** and **2** made via hydrolysis of the protected sugar or directly, mass, UV−vis, and fluorescence spectra confirmed the structure.

Octanol/Water Partition Coefficient. A small amount (∼1 mg) of dry porphyrin was dissolved in 3 mL of 1-octanol by sonication, and 3 mL of distilled water (or pH 4.75 LiAc buffer) was added to the solution. The saturated mixture was shaken vigorously and centrifuged for 10 min to accelerate the separation of the water and organic layers. The absorption of the porphyrin Soret bands in each layer was measured by UV−vis spectroscopy. The ratio of the absorption in 1-octanol over the absorption in water or buffer is the reported octanol/water partition coefficient.

Cell Culture. Cells were maintained in Dulbecco's Modified Eagle Medium (DMEM), 10% bovine calf serum, 1% antimycotic at 37 °C and in 5% CO_2 atmosphere (*31*). For experiments, 2×10^5 cells/mL were seeded in cell culture plates and then allowed to grow for 24 h. For all the experiments involving porphyrins, the conjugate was added to the cells 24 h prior to experiments to allow them to be taken up by the cells.

Fluorescence Imaging Cells. Cells were plated onto cover slips in cell culture dishes. Porphyrins (dissolved in methanol) were added to the cultures to a final concentration of 2−20 μM. Twenty-four hours later, cells were washed twice with PBS (136 mM NaCl, 2.6 mM KCl, 1.4 mM KH_2PO_4, 4.2 mM Na_2HPO_4) and fixed in 4% paraformaldehyde solution in PBS for 20 min at room temperature. The cells were then washed with PBS 5 times (*32*, *33*). The cover slips were mounted in Dako fluorescent mounting medium, put onto slides, air-dried, and then visualized using a Nikon Optiphot 2 fluorescence microscope where images were captured as high quality (>100 kb) JPEG files (excitation: 505−565 nm and emission: 565−685 nm). For comparison and to record cell morphology, images were also captured as JPEG images using a phase contrast light microscope. For each set of experiments, cells were cultured, and the fluorescence images were taken under identical culture and microscopic conditions.

For quantitative studies, the image intensities of the cells in the fluorescence micrographs were calculated by Scientific Image software, developed by Advanced Science and Technology (*34*). This program can analyze images in JPEG format as briefly outlined next.

The red, green, and blue (R, G, B) components of several selected cell regions in the first image were averaged to get (Rc, Gc, Bc). For the same image, several regions of background were selected, and (R, G, B) for the background regions are averaged to get (Rb, Gb, Bb). The background intensity was considered as noise, which was subtracted from the intensity of the cell region. This gives the background adjusted (R1, G1, B1) for the first image. For the second image, (R2, G2, B2) was obtained in the same way. For each image, the absolute intensity, expressed as a (R, G, B) vector, was obtained as the scalar value of the vector. The relative fluorescence intensity between two images was taken as the ratio of the absolute intensity of two images. Additionally, the ratios for the red, green, and blue components of two images can be separately calculated in a straightforward manner. The data were calculated from the original RGB data of the unprocessed images. For publication purposes, the images were enhanced using Microsoft Photo Editor using the same parameters for each set of images.

Photocytotoxicity Assay. Cell viability was quantified by trypan blue exclusion. After various treatments, cells were harvested with trypsin. Trypan blue was added to cells at a concentration of 0.4% w/v. The mixture was incubated at room temperature for 10 min, and trypan blue uptake (counted as dead cells) was determined by counting on a hemacytometer.

Western Blot. Cells were treated with porphyrin for 24 h, rinsed, and irradiated as described in the text. Nine hours after irradiation, cells were washed with cold PBS (136 mM NaCl, 2.6 mM KCl, 1.4 mM KH_2PO_4, 4.2 mM Na_2HPO_4) twice before lysis with RIPA buffer (50 mM Tris-HCL, 1% NP40, 0.25% Na-deoxycholate, 150 mM NaCl, 1 mM EDTA, 1 mM PMSF, 1 μg/mL Aprotinin, leupeptin, pepstatin, 1 mM Na_3VO_4, and NaF). The lysates were gently rocked at 4 °C for 25 min and centrifuged at maximum speed for 10 min, and the supernatant was applied to a Western blot (*35*). Equal amounts of protein were adjusted into gel-loading buffer (50 mM Tris-HCl, pH 6.8; 100 mM dithiothreitol; 2% SDS; 0.1% bromophenol blue; 10% glycerol) and then heated for 5 min at 100 °C prior to separation by SDS−polyacrylamide gel electrophoresis using 8% acrylamide separating gels. After transferring to nitrocellulose membranes (Osmonics), membrane filters were blocked overnight at 4 °C with 5% nonfat dry milk in PBS. The nitrocellulose filters were washed three times for 5 min in PBS with 0.05% tween-20 and then incubated with the anti-PARP antibody for 1 h at room temperature. Anti-mouse IgG conjugated with horseradish peroxidase was used as a secondary antibody. The bands were visualized using an enhanced chemiluminescent detection system (Amersham).

Cell Migration Assay. Cell migration was measured as the ability of cells to migrate through a Biocoat filter (8.0 micron pore size) (*36*). Cells were treated with porphyrin 24 h prior to the assay and kept in the dark. After rinsing and removal of cells from a 60 mm cell culture plate using a balanced salt solution containing 0.5% (w/v) trypsin and 0.2% (w/v) EDTA, 2×10^4 cells in 250 μL of cell culture medium (0.5% serum) was placed in the upper compartment of a Biocoat filter. A total of 750 μL of cell culture medium was placed in the lower compartment of the filter. Cells were irradiated under 13 W fluorescent white light and left to migrate for 18 h. The filters were maintained at 37 °C in a humidified atmosphere containing 95% air and 5% CO_2. After treatment, the filters were removed, and cells that had not migrated through to the underside of the filter were removed from the upper compartment by wiping the filter with a cotton bud. The filters were washed twice with PBS and then incubated in staining buffer Diff-Quik Fixative, Diff-Quik

Solution I, and Diff-Quik Solution II for 0.5 min each at room temperature. The filters were then washed twice in PBS and air-dried. The cells that had migrated to the opposite side of the filter were visualized using a phase contract light microscope, and images were taken.

RESULTS AND DISCUSSION

Synthesis and Characterization. Because of the potential to target various cell types, other S-glycosylated porphyrins have been examined as possible agents for PDT (*29*, *30*). But, one of the goals herein is to develop high-yielding reactions that are general for the appending of any thio-sugar to 5,10,15,20-tetra(pentafluorophenyl)porphyrin ($TPPF_{20}$), which is commercially available and can be routinely made in large quantities either by the Adler (*37*) or Lindsey(*38*) methods. Changing the link between aromatic and sugar moieties from oxygen to sulfur is known to increase the stability of the conjugate to acid hydrolysis. Since sulfur is a weaker Lewis base than oxygen, it has a lower affinity for protons, thus less readily forms the conjugate acid required for the hydrolysis transition state (*39*). The same is true for reactions with glycosidases, as enzymes that act on the corresponding O-analogues do not usually cleave 1-thio saccharides (*39*).

The synthesis begins with $TPPF_{20}$ since the para fluoro group is known to be reactive toward nucleophilic substitution reactions (*40*, *41*), and we have previously exploited this property to make a variety of porphyrin derivatives (*24*). The present work focuses on the preparation of S-glycosylated porphyrins, in which the hydrolytically labile acetal moiety of the sugar is replaced with a functionality that is significantly more stable toward acids, bases, and enzymes. These properties may both increase the selectivity as compared to simple amphipathic compounds and reduce the dosages needed for PDT agents as compared to O-linked saccharides. Two sugar−porphyrin conjugates, **1** ($P\text{-}Glu_4$) and **2** ($P\text{-}Gal_4$), are made as shown in Scheme 2. The synthesis is straightforward, and >85% yields are routinely obtained starting from $TPPF_{20}$ and the thioacetate of the protected sugar in DMF with 20 equiv (∼1%) of diethylamine to deprotect the thiol moiety in situ. Both $P\text{-}Glu_4$ and $P\text{-}Gal_4$ and their protected intermediates were fully characterized. Either the acetate protected or the free sugar can be used in the synthesis of $P\text{-}Glu_4$ and $P\text{-}Gal_4$ (Scheme 2). The protected sugars enhance the reproducibility of the reaction yields and aid in characterization of the products by NMR but necessitate a deprotection step. The removal of the acetate protecting groups with $NaOCH_3$ is quantitative and is followed by neutralization with a pH 7.2 ammonium acetate buffer. A large excess of $NaOCH_3$ should be avoided as it partially cleaves the porphyrin−saccharide conjugate.

The ∼30% broadening of the Soret band and the ∼3 nm red shifts of Q-bands as compared to the starting porphyrin in the UV−vis spectrum of, for example, $P\text{-}Glu_4$ in methanol (Figure 1A) shows that there is some small amount of aggregation even at micromolar concentrations. The hydrophobic porphyrin core surrounded by the hydrophilic sugar moieties likely allows π-stacking of the macrocycles to form dimers or small aggregates. Similar aggregation is observed in water.

The fluorescence intensity of $TPPF_{20}$ is ∼37% of the nonfluorinated analogue, TPP, because of the differences in

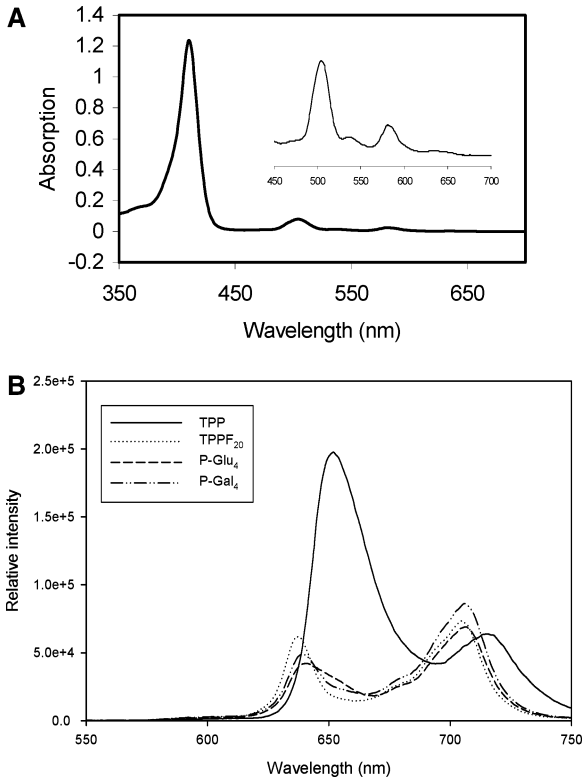

FIGURE 1: (A) UV−vis spectrum of ∼2 μM $P\text{-}Glu_4$ in methanol, where the inset is ×5. (B) Fluorescence emission spectra of TPP, $TPPF_{20}$, $P\text{-}Glu_4$, and $P\text{-}Gal_4$. The concentrations were 0.813, 0.718, 0.360, and 0.336 μM, respectively, in methanol, taken under identical instrumental conditions, and the spectra are normalized to the same molarity.

the energetics of the frontier orbitals and an increase in intersystem crossing to the triplet state. The triplet quantum yield for TPP is 80 ± 10% and for $TPPF_{20}$ is >80% (*12*). The fluorescence intensity of both $P\text{-}Glu_4$ and $P\text{-}Gal_4$ is quenched a further ∼5% as compared to $TPPF_{20}$ under identical instrumental and concentration conditions (Figure 1B). Using fluorescence as an indirect indicator, this observation suggests that $P\text{-}Glu_4$ and $P\text{-}Gal_4$ have even greater quantum yields of triplet than $TPPF_{20}$, and this is likely due to the four sulfur atoms and the heavy atom effect. Of course, these values should only be taken as relative indications of the degrees of the excited-state decay pathway via the triplet manifold. Thus, the quantum yields of singlet oxygen for **1** and **2** are expected to be correspondingly greater as compared to simple TPP derivatives (i.e., the increased number of porphyrins in the triplet excited state will presumably produce more singlet oxygen for a given amount of dye). The photophysical properties of porphyrins and the mechanism of singlet oxygen formation pertaining to PDT have been well-reviewed (*3*, *8*, *13*). Even though the fluorescence quantum yield of these free base porphyrins is ∼10%, the large extinction coefficient ($\sim 2 \times 10^5\ M^{-1}\ cm^{-1}$) and long integration times allows the observation of nanomolar quantities of these dyes by fluorescence microscopy.

These two conjugates are stable to hydrolysis between pH 4.75 and 9. Solutions of both $P\text{-}Glu_4$ and $P\text{-}Gal_4$ in methanol are photochemically stable in refluxing methanol for 6 h under ambient light 21.6 kJ m^{-2} (0.1 mW cm^{-2}) as judged by ESI-MS. This confirms our hypothesis that these conjugates are stable under these conditions. Other saccharide-

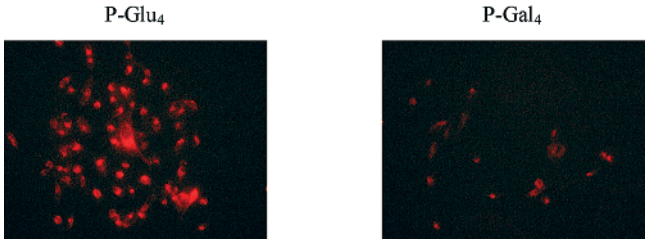

FIGURE 2: P-Glu$_4$ is preferentially taken up by human breast cancer MDA-MB-231 cells over P-Gal$_4$. Cells were treated with 10 μM glycosylated porphyrin for 24 h, rinsed, and fixed with a 4% paraformaldehyde solution. Fluorescence images were taken under identical conditions. R,G,B vector analysis of the unmodified images indicates the average relative fluorescence intensity, taken to be proportional to the extent of conjugate uptake by these cells, is 2.3:1 for P-Glu$_4$/P-Gal$_4$.

appended porphyrins assembled via oxygen linkages are known to be labile under similar conditions (*30*). Photolysis experiments on P-Glu$_4$ indicate little oxidation of the sulfur or cleavage of the sugar from the porphyrin under the conditions used for the treatment of the cells.

There are numerous reports on the correlation of amphipathic character of PDT agents with cell uptake and/or efficacy of PDT (*27*, *42*−*45*). The octanol/water partition coefficients for each derivative are the same in unbuffered water and pH 4.75 buffer (in unbuffered water P-Glu$_4$ is 204 ± 10 and P-Gal$_4$ is 158 ± 20; while in pH 4.75 buffer P-Glu$_4$ is 199 ± 10 and P-Gal$_4$ is 156 ± 10). Since the region around cancer cells is often acidic due to the increase metabolic rate (*8*, *13*, *46*), the unchanged partition coefficients at lower pH indicates that any passive uptake of these compounds by cancer cells will be unaffected. This property arises from the hydrophobic core surrounded by the four hydrophilic groups, the ionization potentials of the hydroxy groups, and somewhat because of the 16 remaining fluoro groups. This is different from porphyrins conjugated to saccharides via an alkane tether with either oxygen or sulfur linkages (*29*, *30*, *47*−*49*). The ~20% difference in the partition coefficient means that P-Glu$_4$ is slightly more lipophilic than P-Gal$_4$, and this may account for a small fraction of the differences noted next.

MDA-MB-231 Breast Cancer Cells. (a) P-Glu$_4$ versus P-Gal$_4$ Selectivity of Cell Uptake. The selective binding of the porphyrin−saccharide conjugates to MDA-MB-231 breast cancer cells was evaluated by fluorescence microscopy. Cells cultured under the same conditions on glass cover slips were incubated with various concentrations of the porphyrin derivatives under identical conditions. After rinsing the unbound compounds from the cells on the cover slips and fixing the cells, fluorescence images of the cells were taken. The observed fluorescence intensity was taken to be proportional to the quantity of porphyrin bound to the cells and was quantified by comparing the integrated RGB vectors for identical areas (see Experimental Procedures).

The fluorescence microscopy images (Figure 2) clearly show that both porphyrin−saccharide conjugates bind to human breast cancer (MDA-MB-231) cells, but these cells take up more than twice as much P-Glu$_4$ than P-Gal$_4$ when incubated with 10 μM solutions for 24 h. The RGB vector analysis, comparing the average values of >20 cells treated with each conjugate from several different experiments,

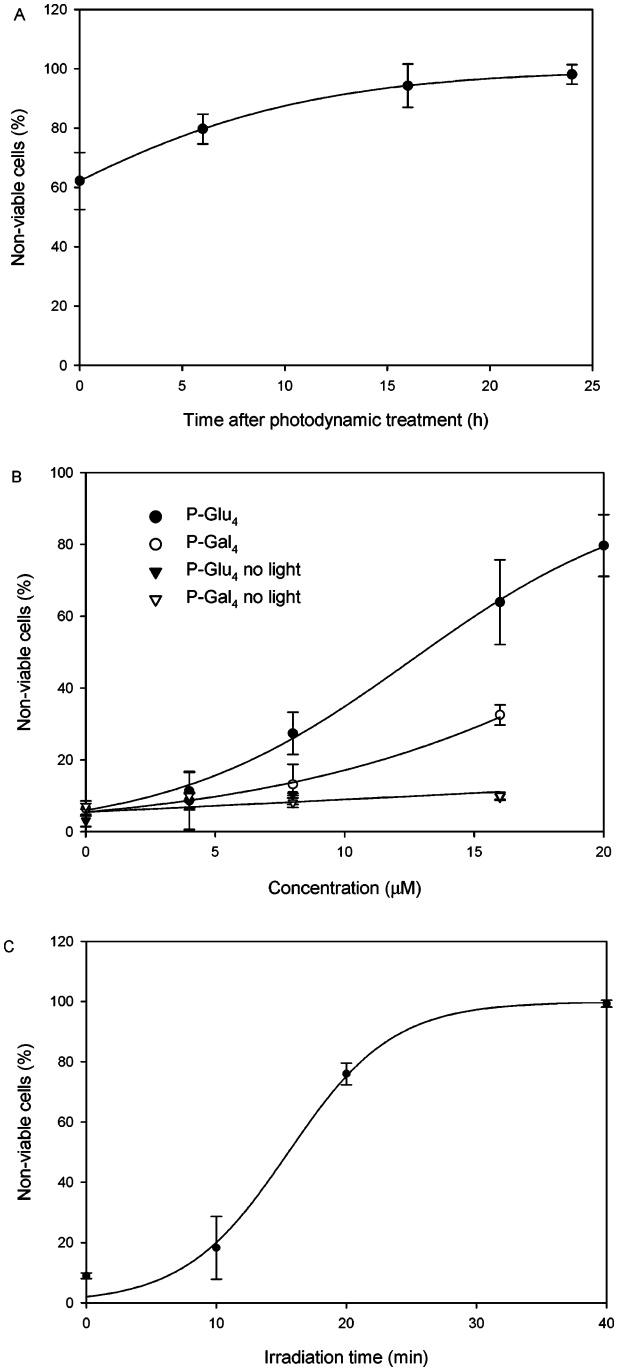

FIGURE 3: Photocytotoxic effects on human breast cancer MDA-MB-231 cells. Nonviable cells were counted with hemacytometer after staining with 0.4% w/v trypan blue. (A) MDA-MB-231 cells were treated with 20 μM P-Glu$_4$ for 24 h, rinsed by exchanging the growth medium, and irradiated under a white 13 W fluorescent light (0.94 mW cm^{-2} for 20 min; 11.28 kJ m^{-2}). The nonviable cells were counted at various lengths of time after photodynamic treatment. (B) MDA-MB-231 cells were treated with various concentrations of P-Glu$_4$ (•) or P-Gal$_4$ (*o*) for 24 h, rinsed by exchanging the growth medium, and irradiated under a white 13 W fluorescent light (0.94 mW cm^{-2} for 20 min; 11.28 kJ m^{-2}). Six hours after photodyamic treatment, nonviable cells were counted. Control experiments with no light show that MDA-MB-231 cells remain viable in the presence of the porphyrin−saccharide conjugates (▼, ▽). (C) MDA-MB-231 cells were treated with 20 μM P-Glu$_4$ for 24 h, rinsed by exchanging the growth medium, and irradiated under a white 13 W fluorescent light (0.94 mW cm^{-2}) for various lengths of time. Six hours after photodynamic treatment, nonviable cells were counted. Each data point represents an average ±SD from at least three independent measurements.

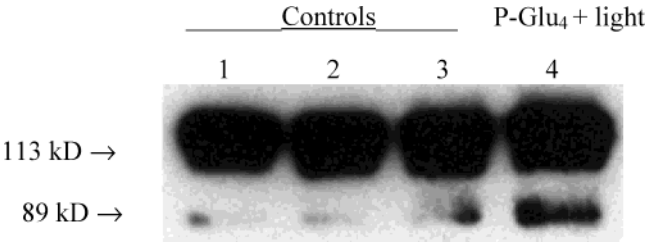

FIGURE 4: Detection of poly-ADP-ribose-polymerase **(**PARP) cleavage in human breast cancer MDA-MB-231 cells as an indication of apoptosis. MDA-MB-231 cells were treated with 20 μM P-Glu$_4$ for 24 h and irradiated with a 13 W fluorescent light (0.27 mW cm^{-2} for 10 min; 1.62 kJ m^{-2}), and 9 h after irradiation, cells were collected and lysed. The supernatant of the lysate was applied to Western blot to detect PARP cleavage. Lane 1: with no irradiation or P-Glu$_4$; lane 2: with irradiation but no P-Glu$_4$; lane 3: with P-Glu$_4$ but no irradiation; and lane 4: with P-Glu$_4$ and irradiation.

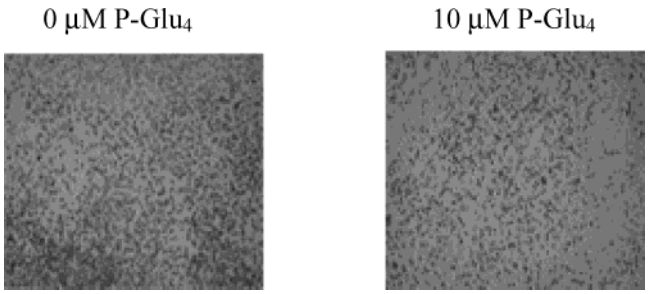

FIGURE 5: Low concentrations of P-Glu$_4$ and low light irradiation inhibit cell migration. Reduced cell migration of human breast cancer MDA-MB-231 cells after nonlethal photodynamic treatment. Cells were treated with 0 or 10 μM P-Glu$_4$ for 24 h and transferred to the Biocoat filters and irradiated under 13 W fluorescent light at 0.25 mW cm^{-2} for 5 min (0.75 kJ m^{-2}). Cells were kept in dark, left to migrate for 18 h, and stained. The images were taken using a phase contrast light microscope.

indicates the uptake of P-Glu$_4$ by MDA-MB-231 is 2.3-fold greater than P-Gal$_4$.

A primary characteristic of malignant cells is an increased uptake of glucose due to increased metabolic activity, and human breast cancer cells are known to have a higher expression and functional level of glucose transporters than normal cells (*50*, *51*). Therefore, the greater binding of P-Glu$_4$ to MDA-MB-231 cells likely arises from the presence of a greater number of glucose transporters than galactose transporters. In addition to the increased active transport, there may be an increased proclivity for these cancer cells to passively absorb conjugates **1** and **2** because of the more acidic environment of cancer cells and increased metabolic rate relative to healthy cells (*46*, *52*−*54*). It has been reported that generally an increasing hydrophobicity increases in vitro activity (*55*). Our observations indicate that the amphipathic nature of the free base porphyrin−sugar conjugates also plays a role in porphyrin incorporation into MDA-MB-231 cells. Neither acetate protected porphyrin intermediates (e.g., **4**) nor TPPF$_{20}$ bind to MDA-MB-231 cancer cells as judged by fluorescence microscopy (Supporting Information); thus, merely increasing lipophilicity does not a priori increase uptake by these cells. The hydrophobic porphyrins either do not enter the cells well and/or there are problems in the delivery these compounds without auxiliary drug delivery formulations such as liposomes.

A previous report found that TPPs bearing eight galactose moieties bound to rat hepatoma (liver cancer) cells (RLC-16), to a much greater extent than the corresponding glucose−porphyrin derivative (*56*). This was expected since there are galactose receptors on this particular cell line but not glucose receptors. Combined with our observations, these results indicate that incorporation of different sugars may direct the porphyrins toward different cell types.

(b) Photocytotoxicity: Necrosis. For cultured breast cancer MDA-MB-231 cells, the P-Glu$_4$ derivative is a more potent mediator of cell death upon illumination with white light than the P-Gal$_4$ derivative, which is consistent with the previous observations on cell uptake/binding. Since cell death can be caused directly by necrosis, and indirectly by initiating apoptosis (*57*), several assays were performed to delineate the extent of each. At 20 μM concentrations of P-Glu$_4$ and using 0.94 mW cm^{-2} of white light for 20 min (11.3 kJ m^{-2}), more than 60% of the cells are necrotic immediately after PDT treatment (within the few minutes it takes to place them under the light contrast microscope, Figure 3A) (*57*). Yet, these two assays also reveal that the number of nonviable cells continues to increase with time until it reaches nearly 100% after 24 h, which implies that under these conditions a secondary process such as apoptosis is causing cell death, vide infra.

Cell viability is porphyrin−saccharide conjugate concentration dependent where the photocytotoxicity of P-Glu$_4$ is approximately 2-fold better than P-Gal$_4$ at 8−16 μM (Figure 3B). The photodynamic response of these cells is also light dose dependent, such that with extended irradiation times, nearly 100% of the cells are dead (Figure 3C). These results confirm those from fluorescence microscope images—glucose−porphyrin conjugates are taken up by human breast cancer MDA-MB-231 cells more than twice as much as the corresponding galactose−porphyrin derivatives.

(c) Photocytotoxicity: Apoptosis. To verify the hypothesis that apoptosis is at least partially the cause of the continued increase in nonviable cells after the cessation of light irradiation (Figure 4), milder conditions were used to decrease the number of initially formed necrotic cells. At

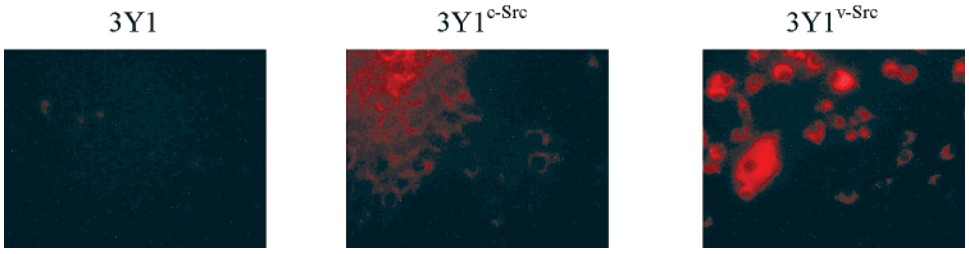

FIGURE 6: P-Glu$_4$ is preferentially taken up by transformed 3Y1^{v-Src} cells as compared to partially transformed 3Y1^{c-Src} cells and nontransformed 3Y1 cells. Cells were treated with 10 μM P-Glu$_4$ for 24 h before fixing with a 4% paraformaldehyde solution. Fluorescence images were taken under identical conditions. The relative fluorescence intensity is 1:2.3:3.2.

the same 20 μM P-Glu$_4$ concentrations, but with 7-fold less total light energy (1.62 kJ m^{-2}; 0.27 mW cm^{-2} for 10 min) than used in the assays shown in Figures 3, cell death is caused at least in part by apoptosis as indicated by a Poly-ADP−ribose-polymerase (PARP) cleavage assay. PARP is one of the best-examined targets of activated caspases and is a common indicator of the action of caspase-3 in apoptosis (*58*). PARP is a DNA repair enzyme whose expression is triggered by DNA strand breaks. In cells undergoing apoptosis, PARP is cleaved from a 113 kD peptide into 24 and 89 kD polypeptides. It appears plausible that cleavage of PARP facilitates the degradation of cellular DNA (*59*), which is a hallmark of apoptosis. Our PARP assay results demonstrate that apoptosis was induced in MDA-MB-231 cells by photodynamic treatment with P-Glu$_4$ (Figure 4). These observations are consistent with other reports (*60*) that lower doses than those needed to produce necrosis are effective in eliciting cell death. This indicates that MDA-MB-231 cell death can be affected even under low light conditions such as found when tumors are further away from the light source and the irradiation has to penetrate through more tissue. Detailed investigations of the role of these porphyrin−saccharide conjugates in affecting apoptosis will be reported elsewhere.

(d) Reduced Cell Migration. It is clear that matastatic tumor cells must retain or increase their ability to migrate and to invade across vessel walls and into tissues (*61*). Decreasing their migration can effectively decrease tumors from spreading (*61*). Using even milder conditions, where the breast cancer MDA-MD-231 cells are kept alive (as indicated by trypan blue exclusion assay) by using still less porphyrin−sugar conjugate and less total light energy (e.g., 10 μM P-Glu$_4$ with 0.75 kJ m^{-2} light irradiation, i.e., 0.25 mW cm^{-2} for 5 min), there is significant inhibition of cell migration. The ability of the cancer to cells migrate from one side of a porous material to the other side (*32*) is much reduced after the treatment with P-Glu$_4$ and irradiation (Figure 5). Control experiments show that P-Glu$_4$ without irradiation or irradiation without P-Glu$_4$ has no effect on cell migration. This result may indicate that lower levels of P-Glu$_4$ in the cells with less light irradiation may damage the membrane or proteins that facilitate or trigger cell migration, thus mitigating aggressiveness. The migration inhibition is porphyrin dose-dependent. Reduced cell migration indicates that the cancer cells are not as aggressive as the untreated MDA-MB-231 cells. This character could slow the tumor spreading to other tissues or organs (*32*) and has clinical relevance when some tumor tissues are too deep for enough light to penetrate to induce necrosis or apoptosis since reduced aggressiveness may facilitate other treatments.

(e) Conclusions on MDA-MB-231 Cells. These observations indicate that the uptake and photodynamic response of the porphyrin−saccharide conjugate by this breast cancer cell line is correlated with the concentration of the compound. The photodynamic response is also correlated with the amount of irradiation with white light. There are no observable effects on cells treated with the conjugates but without light or on cells treated with light but no conjugate. These results also indicate that even at low dosage and low irradiation—such as might be found for central regions of a tumor where the drug has lower uptake and light penetrates less—these compound still may elicit desirable effects such

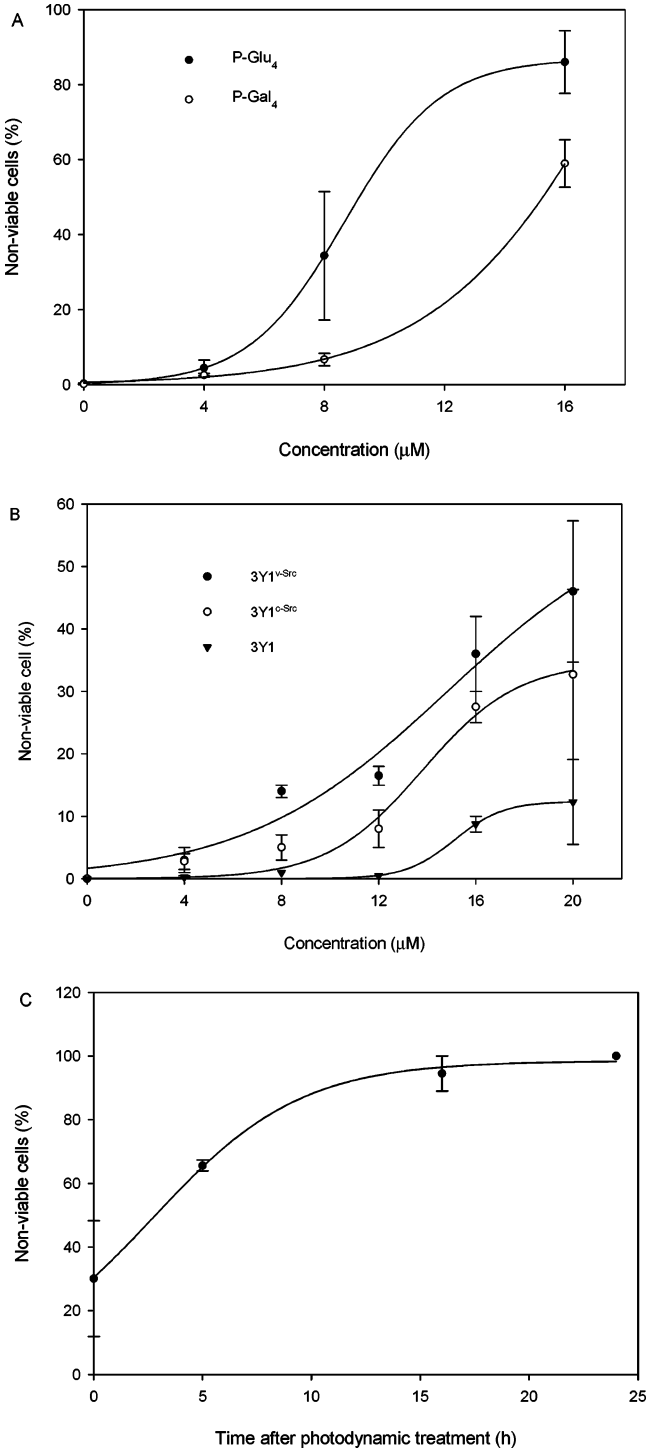

FIGURE 7: (A) Photocytotoxic effects of various concentrations of P-Glu$_4$ and P-Gal$_4$ on 3Y1^{v-Src} cells are compared using 5.76 kJ m^{-2} white light (0.96 mW cm^{-2} from a 13 W fluorescent bulb for 10 min), where nonviable cells were visualized with trypan blue staining 5 h after treatment. (B) The photocytotoxic effects of various concentrations of P-Glu$_4$ on transformed 3Y1^{v-Src}, partially transformed 3Y1^{c-Src}, and normal 3Y1 cells using 3.53 kJ m^{-2} white light (0.84 mW cm^{-2} from a 13 W fluorescent bulb for 7 min), where necrotic cells were visualized with trypan blue staining immediately after treatment. (C) The photocytotoxic effects of 10 μM P-Glu$_4$ on transformed 3Y1^{v-Src} using 11.52 kJ m^{-2} white light (0.96 mW cm^{-2} from a 13 W fluorescent bulb for 20 min). Nonviable cells were counted at various lengths of time after photodynamic treatment. Each data point represents an average ±SD from at least three independent measurements.

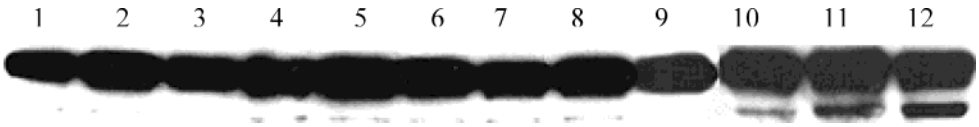

FIGURE 8: Different degrees of PARP cleavage in fully transformed ($3Y1^{v-Src}$), partially transformed ($3Y1^{c-Src}$), and normal (3Y1) rat fibroblasts as indications of apoptosis. 3Y1, $3Y1^{c-Src}$, and $3Y1^{v-Src}$ cells were treated with 8 μM P-Glu_4 for 24 h. Cells were irradiated at 0.84 mW cm^{-2} for 3.5 min (1.76 kJ m^{-2}), and 9 h later the cells were collected and lysed. The supernatant of the lysate was applied to Western blot to detect PARP cleavage. Lane 1: 3Y1 cells with no photodynamic treatment; lane 2: $3Y1^{c-Src}$ cells with no photodynamic treatment; lane 3: $3Y1^{v-Src}$ cells with no photodynamic treatment; lane 4: 3Y1 cells with irradiation but no P-Glu_4; lane 5: $3Y1^{c-Src}$ cells with irradiation but no P-Glu_4; lane 6: $3Y1^{v-Src}$ cells with irradiation but no P-Glu_4; lane 7: 3Y1 cells with P-Glu_4 but no irradiation; lane 8: $3Y1^{c-Src}$ cells with P-Glu_4 but no irradiation; lane 9: $3Y1^{v-Src}$ cells with P-Glu_4 but no irradiation; lane 10: 3Y1 cells with irradiation and P-Glu_4; lane 11: $3Y1^{c-Src}$ cells with irradiation and P-Glu_4; and lane 12: $3Y1^{v-Src}$ cells with irradiation and P-Glu_4.

as apoptosis and reduced aggressiveness. These results support the hypothesis that saccharides may be used to enhance the selectivity of the compound toward a given cell type and can be predicted using a knowledge of the target cell metabolism and/or relative abundance of receptors for a given sugar.

Normal, Partially Transformed, and Fully Transformed 3Y1 Rat Fibroblasts. Overexpression of a tyrosine kinase is a common genetic defect in a variety of human cancers. It was demonstrated previously that 3Y1 rat fibroblasts overexpressing c-Src ($3Y1^{c-Src}$) are partially transformed since elevated expression of the less active c-Src kinase is not sufficient to fully transform cells (*62*). However, when treated with tumor-promoting phorbal esters (*63*), these cells become transformed. Expression of v-Src, which is an activated kinase, fully transforms 3Y1 cells ($3Y1^{v-Src}$) (*64*). Thus, we employed a system of normal (3Y1 rat fibroblasts), partially transformed ($3Y1^{c-Src}$), and fully transformed ($3Y1^{v-Src}$) cells to evaluate the P-Glu_4, and P-Gal_4 conjugates for binding and PDT effects.

(a) Selectivity of Cell Uptake. The three cell types on cover slips were incubated with porphyrin derivatives under identical conditions. After rinsing off the unbound compounds and fixing the cells, the uptake of the porphyrin−saccacharide conjugates by cells was evaluated by fluorescence microscopy, where the observed fluorescence intensity was taken to be proportional to the quantity of porphyrin taken up by the cells, and confirmed by the RGB vector analysis. These studies also show that P-Glu_4 is preferentially absorbed by the transformed $3Y1^{v-Src}$ cells as compared to the absorption of P-Gal_4 (Supporting Information), so we again use the glucose derivative for further investigation. Importantly, neither of the porphyrins are taken up by normal 3Y1 fibroblasts to the extent that they are in the transformed $3Y1^{v-Src}$ cells. The partially transformed $3Y1^{c-Src}$ shows an intermediate uptake (Figures 6 and 7), which indicates that these sugar−appended porphyrins are selective toward tumor over normal cells.[2]

Fluorescence image assays (Figure 6) indicate that the uptake of P-Glu_4 increases in the order of 3Y1 (normal rat fibroblast) < $3Y1^{c-Src}$ (partially transformed cells) < $3Y1^{v-Src}$ (fully transformed cells). The relative affinity of P-Glu_4 toward 3Y1, $3Y1^{c-Src}$, and $3Y1^{v-Src}$ cells is 1:2.3:3.2 according to the relative fluorescence intensity calculated by the Scientific Image program, as described in the Experimental Procedures. This indicates that the tumor-like $3Y1^{v-Src}$ cells have >3-fold greater affinity toward P-Glu_4 than do the corresponding normal cells, further supporting the hypothesis that saccharides can increase the selectivity of porphyrins for tumor cells over normal cells.

For malignant cells, elevated metabolic activity leads to greater uptake of glucose and this is true for $3Y1^{v-Src}$ cells as compared to $3Y1^{c-Src}$ and 3Y1 cells. Thus, glucose uptake is greater due to increased active transport by elevated expression and/or function of glucose transporters. The observed increase in the affinity for P-Glu_4 with increasing degree of cell transformation is consistent with this expectation: $3Y1^{v-Src}$ > $3Y1^{c-Src}$ > 3Y1. In addition to elevated active glucose transport, there may be an increased tendency for tumor (or tumor-like) cells to passively absorb P-Glu_4 because of the faster growth rate and differences in the environment of tumor cells relative to normal cells. The lower pH around cancer cells, for example, may partially protonate free base porphyrins, therefore increasing the hydrophilicity and assisting the cationic porphyrin binding to the cell membrane-containing anionic lipids. The neutral amphipathic porphyrin can cross the membrane or since the cationic porphyrin retains much of its amphipathic nature it may also passively enter the cell. Note that P-Glu_4 is taken up to a greater extent by the $3Y1^{v-Src}$ cells, supporting the hypothesis that the glucose facilitates transport. Thus, the differences in uptake cannot be ascribed solely to the small difference in octanol/water partition coefficients.

(b) Photocytotoxicity: $3Y1^{v-Src}$ > $3Y1^{c-Src}$ >3Y1. Cells from the three different cell lines were treated identically. Various concentrations of P-Glu_4 were incubated with the cells for 24 h, and the medium was changed to remove any unbound conjugate. Then cells were irradiated for 7 min at 0.84 mW cm^{-2} (3.5 kJ m^{-2}). Immediately after irradiation, cells were treated with a 0.4% w/v trypan blue solution for 10 min at room temperature. Blue stained cells were counted as nonviable cells using a light microscope.

The observed phototoxicity of P-Glu_4 on the three cell lines corresponds to their uptake as determined by their fluorescence images. P-Glu_4 has the highest affinity toward $3Y1^{v-Src}$ cells, and ~45% of these cells are rendered nonviable under these PDT conditions using 20 μM conjugate. Consistent with the uptake assays, the percentage of nonviable $3Y1^{c-Src}$ and 3Y1 cells under the same PDT conditions decreases to ~30 and ~10%, respectively (Figure 7).

(c) Photocytotoxicity: Apoptosis. As with the MDA-MB-231 cells, a PARP cleavage assay was used as an indication of apoptosis in all three 3Y1 cell lines post-photodynamic treatment (Figure 8). No PARP cleavage is observed in control experiments on the three 3Y1 cell lines (no irradiation or porphyrin, with irradiation but no porphyrin, or with porphyrin but no irradiation), which indicates that there is

[2] Fluorescence imaging assays demonstrate that normal mouse fibroblast (NIH3T3) do not take up either P-Glu_4 or P-Gal_4.

no apoptotic induction without both P-Glu_4 and light. Detailed analysis of the apoptotic response of these cells to photodynamic treatment with P-Glu_4 will be the subject of a later report.

The cells were incubated with 8 μM P-Glu_4 for 24 h, whereupon the medium was changed just prior to irradiation to ensure that no unbound porphyrins remain in the medium. Cells were irradiated at 0.84 mW cm^{-2} for 3.5 min (1.764 kJ m^{-2}). Nine hours later, the cells were collected and lysed, and the lysate was analyzed by a Western blot. As it is shown in Figure 8, there is no PARP cleavage in normal 3Y1 rat fibroblasts, an intermediate degree of PARP cleavage in the partially transformed $3Y1^{c-Src}$ cells is observed, and the transformed $3Y1^{v-Src}$ cells exhibit the most PARP cleavage.

(d) 3Y1 Conclusions. These results reinforce the MDA-MB-231 results in that the P-Glu_4 conjugate has good selectivity for the transformed cells over normal cells. Both necrosis and apoptosis are a consequence of the photodynamic treatment of the transformed cells and correlate with the extent of P-Glu_4 uptake. The extent of both necrosis and apoptosis increases in the order of fully transformed cells ($3Y1^{v-Src}$) > partially transformed cells ($3Y1^{c-Src}$) > normal rat fibroblasts (3Y1).

CONCLUSION

The formation of saccharide conjugates to porphyrins and related compounds can be accomplished in high yields in one or two steps by using thiosaccharides and a pentafluorophenyl group on the macrocycle. The thio-linker results in a porphyrin−saccharide conjugate that is nonhydrolizable under physiological conditions—enzymatically or by reduced pH. In the present studies, we used the symmetric tetra-substituted $TPPF_{20}$; however, different pentafluorophenyl porphyrin substitution patterns with one to three saccharides may be readily formed by using less than 4 equiv of the thiosugar and chromatographic separation. These later derivatives would have different octanol/water partition coefficients and thus different activities. The significantly enhanced uptake of the P-Glu_4 derivative over the P-Gal_4 derivative by aggressive malignant MDA-MB-231 and the transformed $3Y1^{v-Src}$ cells indicates this is a viable strategy for targeting cancer cells. Importantly, the fact that normal 3Y1 fibroblasts absorbed the P-Glu_4 to a much lesser extent than the transformed $3Y1^{v-Src}$ cells indicates that discrimination between healthy and cancerous cells is achievable by using simple sugars. Furthermore, P-Glu_4 and P-Gal_4 are effective PDT agents as they induce cell death by necrosis and/or apoptosis, depending on the concentration of the conjugate and on the light exposure. At still lower concentrations of the porphyrin and light exposure, cells are rendered less aggressive as indicated by significantly reduced mobility. The apoptosis and mobility observations may indicate that the PDT methodology using P-Glu_4 or P-Gal_4 remains effective even when there is poor light penetration and low concentrations of the porphyrin−saccharide conjugate.

There are a number of reports on the potential of glycosylated porphyrins as PDT agents; however, the major conclusion that can be made is that the complex interplay between structure lipophilicity and the extent of cell binding/uptake differs widely from system to system. The field lacks a set of standardized protocols that make rigorous comparisons of results from different labs difficult if not impossible.

ACKNOWLEDGMENT

This paper is in memory of Marie K. Drain.

SUPPORTING INFORMATION AVAILABLE

Fluorescence images of human breast cancer MDA-MB-231 cells after incubation with nonbinding, hydrophobic porphyrins (compounds **4**, $TPPF_{20}$, tetra(4-carboxyphenyl)porphyrin tetramethyl ester, and tetra(4-methoxyphenyl)porphyrin. Fluorescence images of fully transformed $3Y1^{v-Src}$ rat fibroblasts after incubation with nonbinding, hydrophobic porphyrin **5**. Extinction coefficients for $TPPF_{20}$, P-Glu_4, and P-Gal_4 in various solvents. MALDI-MS for P-Glu_4, and P-Gal_4. Fluorescence image of normal mouse fibroblast NIH3T3 with P-Glu_4. This material is available free of charge via the Internet at http://pubs.acs.org.

REFERENCES

1. Drain, C. M., Christensen, B., and Mauzerall, D. C. (1989) Photogating of ionic currents across a lipid bilayer, *Proc. Natl. Acad. Sci. U.S.A. 86*, 6959−6962.
2. Drain, C. M., and Mauzerall, D. C. (1992) Photogating of ionic currents across lipid bilayers: Hydrophobic ion conductance by an ion chain mechanism, *Biophys. J. 63*, 1556−1563.
3. MacDonald, I. J., and Dougherty, T. J. (2001) Basic principles of photodynamic therapy, *J. Porphyrins Phthalocyanines 5*, 105−129.
4. Neurath, A. R., Strick, N., and Debnath, A. K. (1995) Structural requirements for and consequences of an antiviral porphyrin binding to the V3 loop of the human immunodeficiency virus (HIV-1) envelope glycoprotein gp120, *J. Mol. Recog. 8*, 345−357.
5. Vzorov, A. N., Dixon, D. W., Trommel, J. S., Marzilli, L. G., and Compans, R. W. (2002) Inactivation of human immunodeficiency virus type 1 by porphyrins, *Antimicrob. Agents Chemother. 46*, 3917−3925.
6. Pandey, R. K. (2000) Recent advances in photodynamic therapy, *J. Porphyrins Phthalocyanines 4*, 368−373.
7. Sternberg, E. D., Dolphin, D., and Bruckner, C. (1998) Porphyrin-based photosensitizers for use in photodynamic therapy, *Tetrahedron 54*, 4151−4202.
8. Bonnett, R. (1995) Photosensitizers of the porphyrin and phthalocyanine series for photodynamic therapy, *Chem. Soc. Rev.* 19−33.
9. Moor, A. C. E. (2000) Signaling pathways in cell death and survival after photodynamic therapy, *J. Photochem. Photobiol., B 57*, 1−13.
10. Mody, T. D. (2000) Pharmaceutical development and medical applications of porphyrin-type macrocycles, *J. Porphyrins Phthalocyanines 4*, 362−367.
11. Jori, G. (1996) Tumor photosensitizers: approaches to enhance the selectivity and efficiency of photodynamic therapy, *J. Photochem. Photobiol., B 36*, 87−93.
12. Yang, S. I., Seth, J., Strachan, J.-P., Gentlemann, S., Kim, D., Holten, D., Lindsey, J. S., and Bocian, D. F. (1999) Ground- and excited-state electronic properties of halogenated tetraarylporphyrins. Tuning the building blocks for porphyrin-based photonic devices, *J. Porphyrins Phthalocyanines. 3*, 117−147.
13. Dougherty, T. J. (1993) Yearly review photodynamic therapy, *Photochem. Photobiol. 58*, 895−900.
14. Granville, D. J., and Hunt, D. W. C. (2000) Porphyrin-mediated photosensitization—Taking the apoptosis fast lane, *Curr. Opin. Drug Discovery Dev. 3*, 232−243.
15. Salva, K. A. (2002) Photodynamic therapy; Unapproved uses, dosages, or indications, *Clin. Dermat. 20*, 571−581.
16. Mauzerall, D. C., and Drain, C. M. (1992) Photogating of ionic currents across lipid bilayers: Electrostatics of ions and dipoles inside the membrane, *Biophys. J. 63*, 1544−1555.

17. Gong, X., Milic, T., Xu, C., Batteas, J. D., and Drain, C. M. (2002) Preparation and characterization of porphyrin nanoparticles, *J. Am. Chem. Soc. 124*, 14290−14291.
18. Hombrecher, H. K., and Schell, C. (1997) Carbohydrate substituted porphyrins. Synthesis, characterization, and lipoprotein binding properties, *Carbohydr. Polym. 34*, 422−423.
19. Sol, V., Blais, J. C., Carre, V., Granet, R., Guilloton, M., Spiro, M., and Krausz, P. (1999) Synthesis, spectroscopy, and photocytotoxicity of glycosylated amino acid porphyrin derivatives as promising molecules for cancer phototherapy, *J. Org. Chem. 64*, 4431−4444.
20. Schell, C., and Hombrecher, H. K. (1999) Synthesis and investigation of glycosylated mono- and diarylporphyrins for photodynamic therapy, *Bioorg. Med. Chem. 7*, 1857−1865.
21. Mikata, Y., Onchi, Y., Tabata, K., Ogura, S.-i., Okura, I., Ono, H., and Yano, S. (1998) Sugar-dependent photocytotoxic property of tetra- and octa-glycoconjugated tetraphenylporphyrins, *Tetrahedron Lett. 39*, 4505−4508.
22. Maillard, P., Vilain, S., Huel, C., and Momenteau, M. (1994) Efficient preparation of the α,α,α,α-atropoisomer of meso-tetrakis-[2-(2,3,4,6-tetraacetyl-*O*-β-glucosyl)phenyl]porphyrin, *J. Org. Chem. 59*, 2887−2890.
23. Chen, X., and Drain, C. M. (2004) Photodynamic therapy using carbohydrate conjugated porphyrins, *Drug Des. Rev.—Online 3*, *1*, 215−234, http://www.bentham.org/ddro/.
24. Pasetto, P., Chen, X., Drain, C. M., and Franck, R. W. (2001) Synthesis of hydrolytically stable porphyrin C- and S-glycoconjugates in high yields, *Chem. Commun.*, 81−82.
25. Brown, R. S., and Wahl, R. L. (1993) Overexpression of Glut-1 glucose transporter in human breast cancer. An immunohistochemical study, *Cancer 72*, 2979−2985.
26. Sharon, M., and Lis, H. (1989) Lectins as cell recognition molecules, *Science 246*, 227−234.
27. Cornia, M., Valenti, C., Capacchi, S., and Cozzini, P. (1998) Syntheis, characterization, and conformational studies of lipophilic, amphiphilic, and water-soluble C-glyco-conjugated porphyrins, *Tetrahedron 54*, 8091−8106.
28. Cornia, M., Menozzi, M., Ragg, E., Mazzini, S., Scarafoni, A., Zanardi, F., and Casiraghi, G. (2000) Synthesis and utility of novel C-meso-glycosylated metalloporphyrins, *Tetrahedron 56*, 3977−3983.
29. Sylvain, I., Benhaddou, R., Carre, V., Cottaz, S., Driguez, H., Granet, R., Guilloton, M., and Krausz, P. (1999) Synthesis and biological evaluation of thioglycosylated *meso*-arylporphyrins, *J. Porphyrins Phthalocyanines 3*, 1−4.
30. Sylvain, I., Zerrouki, R., Granet, R., Huang, Y. M., Lagorce, J.-F., Guilloton, M., Blais, J.-C., and Krausz, P. (2002) Synthesis and biological evaluation of thioglycosylated porphyrins for an application in photodynamic therapy, *Bioorg. Med. Chem. 10*, 57−69.
31. Hornia, A., Lu, Z., Sukezane, T., Zhong, M., Joseph, T., Frankel, P., and Foster, D. A. (1999) Antagonistic effects of protein kinase Cα and δ on both transformation and phospholipase D activity mediated by the epidermal growth factor receptor, *Mol. Cell Biol. 19*, 7672−7680.
32. Shen, Y., Xu, L., and Foster, D. A. (2001) Role for phospholipase D in receptor-mediated endocytosis, *Mol. Cell Biol. 21*, 595−602.
33. Willingham, M. C., and Pastan, I. (1985) *An Atlas of Immunofluorescence in Cultured Cells*, Academic Press, Orlando.
34. Qian, G. (2003) Advanced Science and Technology, http://www.howardast.com, New York.
35. Lu, Z., Hornia, A., Joseph, T., Sukezane, T., Frankel, P., Zhong, M., Bychenok, S., Xu, L., Feig, L. A., and Foster, D. A. (2000) Phospholipase D and RalA cooperate with the epidermal growth factor receptor to transform 3Y1 rat fibroblasts, *Mol. Cell Biol. 20*, 462−467.
36. Shen, Y., Zheng, Y., and Foster, D. A. (2002) Phospholipase D2 stimulates cell protrusion in v-Src-transformed cells, *Biochem. Biophys. Res. Commun. 293*, 201−206.
37. Adler, A. D., Longo, F. R., Finarelli, J. D., Goldmacher, J., Assour, J., and Korsakoff, L. (1967) A simplified synthesis of meso-tetraphenylporphin, *J. Org. Chem. 32*, 476−476.
38. Lindsey, J. S., Schreiman, I. C., Hsu, H. C., Kearney, P. C., and Marguerettaz, A. M. (1987) Rothemund and Adler−Longo reactions revisited: synthesis of tetraphenylporphyrins under equilibrium conditions, *J. Org. Chem. 52*, 827−836.
39. Defaye, J., and Gelas, J. (1991) Thio-oligosaccharides: Their Synthesis and Reactions with Enzymes, in *Studies in Natural Products Chemistry* (Atta-ur-Rahman, Ed.) pp 315−357, Elsevier Science Publishers B. V., Amsterdam.
40. Shaw, S. J., Edwards, C., and Boyle, R. W. (1999) Regioselective synthesis of multifunctionalised porphyrins—coupling of mono-(pentafluorophenyl)porphyrins to electrophiles, *Tetrahedron Lett. 40*, 7585−7586.
41. Shaw, S. J., Elgie, K. J., Edwards, C., and Boyle, R. W. (1999) Mono-(pentafluorophenyl)porphyyrins—Useful intermediates in the regioselective synthesis of multifunctionalised porphyrins, *Tetrahedron Lett. 40*, 1595−1596.
42. Momenteau, M., Oulmi, D., Maillard, P., and Croisy, A. F. (1994) In vitro photobiological activity of a new series of photosensitizers: the glycoconjugated porphyrins, *Proc. SPIE 2325 Photodynamic Therapy of Cancer II*, 13−23.
43. Adams, K. R., Berenbaum, M. C., Bonnett, R., Nizhnik, A. N., Salgado, A., and Valles, M. A. (1992) Second generation tumour photosensitisers: the synthesis and biological activity of octaalkyl chlorins and bacteriochlorins with graded amphiphilic character, *J. Chem. Soc., Perkin Trans. 1*, 1465−1470.
44. Oulmi, D., Maillard, P., Guerquin-Kern, J.-L., Huel, C., and Momenteau, M. (1995) Glycoconjugated porphyrins. 3. Synthesis of flat amphiphilic mixed meso-(glycosylated-aryl)arylporphyrins and mixed meso-(glycosylated-aryl)alkylporphyrins bearing some mono- and disaccharide groups, *J. Org. Chem. 60*, 1554−1564.
45. Drain, C. M., Gong, X., Ruta, V., Soll, C. E., and Chicoineau, P. F. (1999) Combinatorial synthesis and modification of functional porphyrin libraries: identification of new, amphipathic motifs for biomolecule binding, *J. Comb. Chem. 1*, 286−290.
46. Maziere, J. C., Santus, R., Morliere, P., Reyftmann, J. P., Candide, C., Mora, L., Salmon, S., Maziere, C., Gatt, S., and Dubertret, L. (1990) Cellular uptake and photosensitizing properties of anticancer porphyrins in cell membranes and low- and high-density lipoproteins, *J. Photochem. Photobiol., B 6*, 61−68.
47. Bourhim, A., Gaud, O., Granet, R., Krausz, P., and Spiro, M. (1993) Synthesis of new glycosylated porphyrin derivatives with a hydrocarbon spacer arm, *Synlett*, 563−564.
48. Gaud, O., Granet, R., Kaouadji, M., Krausz, P., Blais, J.-C., and Bolbach, G. (1996) Synthese et analyse structurale de nouvelles *meso*-arylporphyrines glycosylees en vue de l'application en phototherapie des cancers, *Can. J. Chem. 74*, 481−499.
49. Carre, V., Gaud, O., Sylvain, I., Bourdon, O., Spiro, M., Blais, J., Granet, R., Krausz, P., and Guilloton, M. (1999) Fungicidal properties of *meso*-arylglycosylporphyrins: influence of sugar substituents on photoinduced damage in the yeast *Saccharomyces cerevisia*, *J. Photochem. Photobiol., B 48*, 57−62.
50. Grover-McKay, M., Walsh, S. A., Seftor, E. A., Thomas, P. A., and Hendrix, M. J. (1998) Role for glucose transporter 1 protein in human breast cancer, *Pathol. Oncol. Res. 4*, 115−120.
51. Younes, M., Brown, R. W., Mody, D. R., Fernandez, L., and Laucirica, R. (1995) GLUT1 expression in human breast carcinoma: correlation with known prognostic markers, *Anticancer Res. 15*, 2895−2898.
52. Brault, D. (1990) Physical chemistry of porphyrins and their interactions with membranes: the importance of pH, *J. Photochem. Photobiol., B 6*, 79−86.
53. Bohmer, R. M., and Morstyn, G. (1985) Uptake of hematoporphyrin derivative by normal and malignant cells: effect of serum, pH, temperature, and cell size, *Cancer Res. 45*, 5328−5334.
54. Friberg, E. G., Cunderlikova, B., Pettersen, E. O., and Moan, J. (2003) pH effects on the cellular uptake of four photosensitizing drugs evaluated for use in photodynamic therapy of cancer, *Cancer Lett. 195*, 73−80.
55. Pandey, R. K., and Zheng, G. (2000) Porphyrins as photosensitizers in photodynamic therapy, in *The Porphyrin Handbook* (Kadish, K. M., Smith, K. M., and Guilard, R., Eds.) pp 157−230, Academic Press, New York.
56. Fujimoto, K., Miyata, T., and Aoyama, Y. (2000) Saccharide-directed cell recognition and molecular delivery using macrocyclic saccharide clusters: masking of hydrophobicity to enhance the saccharide specificity, *J. Am. Chem. Soc. 122*, 3558−3559.
57. Kroemer, G., Dallaporta, B., and Resche-Rigon, M. (1998) The mitochondrial death/life regulator in apoptosis and necrosis, *Annu. Rev. Physiol. 60*, 619−642.

58. Yu, S.-W., Wang, H., Poitras, M. F., Coombs, C., Bowers, W. J., Federoff, H. J., Poirier, G. G., Dawson, T. M., and Dawson, V. L. (2002) Mediation of poly(ADP-ribose) polymerase-1-dependent cell death by apoptosis-inducing factor, *Science 297*, 259−263.
59. de Murcia, G., and Menissier de Murcia, J. (1994) Poly(ADP-ribose) polymerase: a molecular nick-sensor, *Trends Biochem. Sci. 19*, 172−176.
60. Oleinick, N. L., Morris, R. L., and Belichenko, I. (2002) The role of apoptosis in response to photodynamic therapy: what, where, why, and how, *Photochem. Photobiol. Sci. 1*, 1−21.
61. Ridley, A. J., Schwartz, M. A., Burridge, K., Firtel, R. A., Ginsberg, M. H., Borisy, G., Parsons, J. T., and Horwitz, A. R. (2003) Cell migration: integrating signals from front to back, *Science 302*, 1704−1709.
62. Zhong, M., Joseph, T., Jackson, D., Beychenok, S., and Foster, D. A. (2002) Elevated phospholipase D activity induces apoptosis in normal rat fibroblasts, *Biochem. Biophys. Res. Commun. 298*, 474−477.
63. Zhong, M., Lu, Z., and Foster, D. A. (2002) Downregulating PKCδ provides a PI3K/Akt-indepentdent survival signal that overcomes apoptotic signals generated by c-Src overexpression, *Oncogene 21*, 1071−1078.
64. Zhong, M., Shen, Y., Zheng, Y., Joseph, T., Jackson, D., and Foster, D. A. (2003) Phospholipase D prevents apoptosis in v-Src-tranformed rat fibroblasts and MDA-MB-231 breast cancer cells, *Biochem. Biophys. Res. Commun. 302*, 615−619.

BI049272V